# The N-Terminus of the Regulatory Chain of *Escherichia coli* Aspartate Transcarbamoylase Is Important for both Nucleotide Binding and Heterotropic Effects†

Jessica B. Sakash and Evan R. Kantrowitz*

*Department of Chemistry, Merkert Chemistry Center, Boston College, Chestnut Hill, Massachusetts 02167*

*Received August 25, 1997; Revised Manuscript Received October 27, 1997*⊗

ABSTRACT: X-ray crystallographic studies indicate that the N-terminal region of the regulatory chain in *Escherichia coli* aspartate transcarbamoylase resides close to the effector binding site. The proximity of the N-terminal region to the binding site suggests it may be important for nucleotide binding and, therefore, the heterotropic mechanism. The N-terminal region of the structure is not well-defined since the electron density in this region is weak, indicating a flexible and mobile region. Furthermore, alanine scanning mutagenesis of residues 2−7 indicated that the N-terminal region may be involved in nucleotide binding and the heterotropic mechanism, especially, UTP recognition [Dembowski, N., and Kantrowitz, E. R. (1994) *Protein Eng. 7,* 673−679]. In order to investigate further the role of the N-terminal region in the heterotropic mechanism, the first 10 N-terminal residues of the regulatory chain were deleted using site-specific mutagenesis. This mutant enzyme was compared to the wild-type enzyme, and both solubility and functional differences were observed. The mutant enzyme forms an insoluble aggregate which can be solubilized by the addition of nucleotides, such as CTP, suggesting that the exposed nucleotide binding site is involved in aggregate formation. Kinetic analyses of the mutant enzyme showed a lower maximal velocity and slightly lower aspartate affinity. Apparent binding constants determined for CTP, ATP, UTP, and CTP in the presence of UTP suggest the heterotropic response is also altered. This study suggests that the N-terminal region of the regulatory subunit is important for controlling nucleotide binding, creating the high-affinity and low-affinity effector binding sites, and coupling the binding sites within the regulatory dimer.

Aspartate transcarbamoylase (EC 2.1.3.2) is an allosteric enzyme which catalyzes the committed step of pyrimidine biosynthesis. The enzyme is regulated homotropically by the substrate L-aspartate (*11*) and heterotropically by the nucleotide effectors ATP, CTP (*11*), and UTP in the presence of CTP (*34*).

The *Escherichia coli* enzyme is a dodecamer composed of six catalytic chains (c) of $M_r$ 34 000 and six regulatory chains (r) of $M_r$ 17 000. The catalytic chains associate to form two catalytic trimers ($2c_3$), and the regulatory chains associate to form three regulatory dimers ($3r_2$), all of which assemble to form the holoenzyme. Each catalytic chain contains two domains, the aspartate domain and the carbamoyl phosphate domain; the active sites are located at the interface between adjacent catalytic chains of the trimer (*17*, *22*, *26*, *33*). Each regulatory chain also contains two domains: the zinc domain and the allosteric domain. The nucleotide effectors bind to the allosteric domain 60 Å from the active site. CTP and ATP bind to the same site on the regulatory chain based on kinetics (*12*, *19*), binding studies (*4*), and analysis of the structure (*13*, *14*, *30*).

The allosteric domain in the regulatory dimer is formed by a 10 strand antiparallel $\beta$-sheet flanked on one side by a row of α-helices (see Figure 1). The nucleotide binding site is located on the other side of the $\beta$-sheet, protected only by the unstructured, flexible region consisting of the first 10 N-terminal amino acids. The importance of this N-terminal region of the regulatory chain has been discussed due to its proximity to the nucleotide binding site (*15*, *16*, *30*). The structure and interactions of the N-terminal region were difficult to establish due to the weak electron density of this region in X-ray crystallographic studies. Honzatko (*15*) proposed that the N-terminal region has several interactions with the nucleotide effectors and might bring together the two allosteric binding sites of the regulatory dimer; however, specific interactions could not be assigned. A later study by Stevens et al. (*30*) showed that the nucleotide cavity undergoes a slight expansion in the presence of CTP and ATP, the expansion being more pronounced with the latter. For this alteration, most apparent was the movement of Ala-11r[1] and Ile-12r which are located at the beginning of the

† This work was supported by Grant GM26237 from the National Institute of General Medical Sciences.

* To whom all correspondence should be addressed.

⊗ Abstract published in *Advance ACS Abstracts,* December 15, 1997.

[1] "r" is appended to the residue number to indicate the regulatory chain. $\Delta(1-10)r_2$ is the mutant regulatory dimer in which the 10 N-terminal amino acids have been deleted; $(c_3)_2(\Delta(1-10)r_2)_3$ is the mutant holoenzyme in which the 10 N-terminal amino acids of the regulatory chain have been deleted; $T^{ATP}$ signifies the T state of the enzyme with ATP bound to the regulatory site; $T^{CTP}$ signifies the T state of the enzyme with CTP bound to the regulatory site (*30*).

S0006-2960(97)02102-8 CCC: $15.00 
Published on Web 01/06/1998

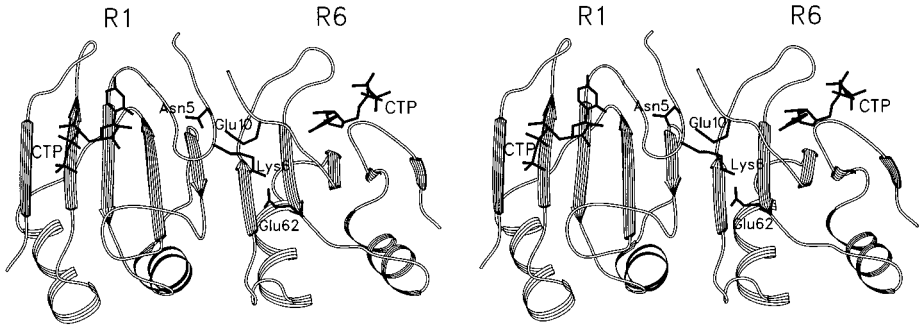


FIGURE 1: Stereoview of the allosteric domains of a regulatory dimer (R1−R6) along the 2-fold axis (*16*). The 10-strand antiparallel $\beta$-sheet flanked by a row of α-helices on one side and the unstructured N-terminal region on the other is shown with CTP bound. This figure was drawn with SETOR (*8*).

S1′ $\beta$-strand. Val-9r and Glu-10r appear to move toward ATP in the $T^{ATP}$ structure but not toward CTP in the $T^{CTP}$ structure.

Kosman et al. (*16*) proposed that the N-terminal region exists in an extended conformation. In this arrangement, there would exist a direct interaction between residues of the N-terminal region and CTP; specifically, the backbone carbonyl of Val-9r forms a hydrogen bond with the 2′-OH of CTP. It was proposed that three additional interactions exist across the R1−R6[2] dimer interface. The main chain NH of Asn-5 (R1) donates a hydrogen bond to the carbonyl oxygen of Gln-8 (R6), and the main chain NH of Lys-6 (R1) has a charge-polar interaction with a side chain oxygen of Glu-10 (R6). The third interaction exists between the main chain carbonyl oxygen and the $\epsilon$-amino group of Lys-6 (R1) with the main chain NH of Gln-8 (R1) and a carboxylate oxygen of Glu-62 (R6), respectively. Kosman et al. (*16*) suggested there may be an important relationship between the N-terminus and the 80r′s loop of the R1 chain because a charge-polar interaction is observed between the side chain oxygen of Tyr-89 and the amino terminus. It is proposed that this charge-polar interaction stabilizes the 80r′s loop which is displaced upon nucleotide binding.

Alanine scanning mutagenesis performed along residues Thr-2r to Leu-7r further elucidated the role of the N-terminal region (*7*). Results suggested that Lys-6r was important for the heterotropic mechanism while several of the residues, His-3r, Asp-4r, Asn-5r, and Lys-6r, were important for UTP inhibition of the enzyme both in the absence and in the presence of CTP at pH 7.0. In this study, we have deleted the first 10 residues of the N-terminus of the regulatory chain in order to determine the importance of its function for aspartate transcarbamoylase. The mutation was created by site-specific mutagenesis, the mutant enzyme was expressed in *E. coli*, and the effects of this mutation on the kinetic parameters of the enzyme were determined.

## EXPERIMENTAL PROCEDURES

### *Materials*

Agarose, ATP, CTP, UTP, L-aspartate, *N*-carbamoyl-DL-aspartate, 2-mercaptoethanol, imidazole, isopropyl-$\beta$-thiogalactosidase, potassium dihydrogen phosphate, sucrose, and uracil were obtained from Sigma. Q-Sepharose Fast Flow was purchased from Pharmacia. Ampicillin, Tris, restriction endonucleases, Sequenase DNA sequencing kit, and T4 DNA ligase were obtained from Amersham/USB and were used according to the manufacturer's recommendations. Sodium dodecyl sulfate was purchased from Bio-Rad. Carbamoyl phosphate dilithium salt, obtained from Sigma, was purified before use by precipitation from 50% (v/v) ethanol and was stored desiccated at −20 °C (*10*). Casamino acids, yeast extract, and tryptone were obtained from Difco. Ammonium sulfate, urea, and electrophoresis grade acrylamide were purchased from ICN Biomedicals. Antipyrine was obtained from Kodak. The DNA oligomer used for the mutagenesis was purchased from Operon Technology, Inc; the Muta-Gene T7 enzyme pack used for the mutagenesis was purchased from Bio-Rad.

*Strains.* The *E. coli* strain MV1190 [Δ(*lac-proAB*), *supE, thi*, Δ(*sri-recA*)306::Tn10(tet$^r$)/F′ *traD36*, *proAB*, *lacI*$^q$, *lacZ*ΔM15], phagemid pUC119, and the M13 phage M13K07 were obtained from J. Messing. EK1104 [F$^-$ *ara*, *thi*, Δ*pro-lac*, Δ*pyrB*, *pyrF*$^{\pm}$, *rpsL*] was previously constructed (*23*). A version of EK1104 which had an inducible gene for T7 DNA polymerase on the chromosome, EK1595 [F$^-$ *ara*, *thi*, Δ(*pro-lac*), Δ*pyrB*, *pyrF*$^{\pm}$, *rpsL*, λDE3], was constructed by introduction of the λDE3 prophage using the λDE3 lysogenation kit from Novagen, Inc.

### *Methods*

*Site-Specific Mutagenesis.* Mutagenesis to insert a *Nde*I restriction endonuclease site between codons 10 and 11 in the *pyrI* gene was performed on single-stranded DNA containing the *pyrBI* operon using the method of Kunkel (*18*). The necessary uracil-containing single-stranded DNA was obtained by infection of *E. coli* strain CJ236 containing the phagemid pEK152 (*2*) with the helper phage M13K07 (*32*). The phagemid pEK152 does not contain an *Nde*I restriction site; therefore, mutant candidates were screened first for the insertion of the *Nde*I restriction site by treatment with *Nde*I. Once a candidate was identified, the smaller *Nde*I−*Eco*RI fragment was isolated and mixed with the larger *Nde*I−*Eco*RI fragment from pEK79, which contained a *Nde*I restriction site at the start of the *pyrI* gene. The two fragments were treated with DNA ligase, and the resulting phagemid, pEK303, contained a deletion corresponding to amino acids 1−10 of the *pyrI* gene product. Single-stranded DNA isolated from phagemid candidates after coinfection with the helper phage M13K07 (*32*) was sequenced (*27*). An expression phagemid, pEK330, to produce the Δ(1−10)

[2] The regulatory chains R1 and R6 comprise one regulatory dimer, while the chains R2 and R4, and R3 and R5 comprise the other two dimers.

regulatory chain under control of the T7 promoter was created by mixing the larger *Nde*I−*Eco*RI fragment of pET23a (*31*) with the smaller *Nde*I−*Eco*RI fragment of pEK303; treatment with DNA ligase resulted in phagemid pEK330.

*Overexpression and Purification of the $(c_3)_2(\Delta(1-10)r_2)_3$ Holoenzyme.* The $(c_3)_2(\Delta(1-10)r_2)_3$ holoenzyme was expressed under control of the *pyrBI* promoter. Strain EK1104 with the phagemid pEK303 was cultured at 37 °C with agitation in M9 media (*21*) containing 0.5% casamino acids, 12 $\mu$g/mL uracil, and 150 $\mu$g/mL ampicillin. After 24 h of growth, the cells were harvested and resuspended in 0.1 M Tris-HCl buffer, pH 9.2, followed by sonication to lyse the cells. Analysis of the supernatant and precipitated cell debris by nondenaturing polyacrylamide gel electrophoresis (*5*, *24*) indicated that the precipitate contained mutant holoenzyme and the supernatant contained catalytic trimer and trace amounts of holoenzyme. Solubilization and purification of the $(c_3)_2(\Delta(1-10)r_2)_3$ holoenzyme from cell debris were difficult, so an alternative purification method was developed.

In another approach, the $\Delta(1-10)$ regulatory chain was expressed under control of the T7 promoter, and the holoenzyme was reconstituted in the presence of the catalytic subunit. Strain EK1595 containing phagemid pEK330 was cultured at 37 °C with agitation in M9 media (*21*) containing 0.5% casamino acids, 30 $\mu$g/mL uracil, and 150 $\mu$g/mL ampicillin. Induction of the T7 polymerase was achieved by addition of 0.4 mM IPTG when the $Abs_{560}$ of the culture was 1.0. After further growth for 4 h, the cells were harvested and resuspended in 50 mM Tris−acetate buffer, 2 mM 2-mercaptoethanol, and 0.1 mM zinc acetate, pH 9.2, and were lysed by sonication.

Crude cell extract containing the $\Delta(1-10)r_2$ was mixed with crude cell extract of the wild-type $c_3$. Upon incubation of the mixture at 4 °C in 50 mM Tris−acetate buffer, 2 mM 2-mercaptoethanol, and 0.1 mM zinc acetate at pH 8.3, a white precipitate formed. Analysis of the supernatant by nondenaturing polyacrylamide gel electrophoresis and sodium dodecyl sulfate electrophoresis (SDS−PAGE) (*20*) indicated only trace amounts of the $(c_3)_2(\Delta(1-10)r_2)_3$ holoenzyme. The precipitate was characterized by SDS−PAGE and nondenaturing PAGE and found to be a mixture of $(c_3)_2(\Delta(1-10)r_2)_3$ holoenzyme and high molecular weight aggregates. The $(c_3)_2(\Delta(1-10)r_2)_3$ precipitate was solubilized in 50 mM Tris−acetate buffer, 2 mM 2-mercaptoethanol, and 3 mM CTP at pH 8.3; nondenaturing PAGE indicated there was a mixture of $(c_3)_2(\Delta(1-10)r_2)_3$ holoenzyme and high molecular weight aggregates.

Separation of the $(c_3)_2(\Delta(1-10)r_2)_3$ holoenzyme from high molecular weight aggregates was performed using a 10−30% sucrose gradient in 50 mM Tris−acetate buffer, 2 mM 2-mercaptoethanol, and 3 mM CTP at pH 8.3. Samples prepared in 50 mM Tris−acetate buffer, 2 mM 2-mercaptoethanol, and 3 mM CTP at pH 8.3 were overlaid onto the gradient; ultracentrifugation was performed in a Beckman Ti55 swinging-bucket rotor at 45 000 rpm at 10 °C for 5.5 h. Each sample was fractionated and analyzed for protein by the Bio-Rad version of Bradford's dye binding assay (*3*) and for $(c_3)_2(\Delta(1-10)r_2)_3$ holoenzyme by nondenaturing gel electrophoresis. The fractions containing the $(c_3)_2(\Delta(1-10)r_2)_3$ holoenzyme were pooled and dialyzed against 50 mM Tris−acetate buffer, 2 mM 2-mercaptoethanol, and 2 mM CTP at pH 8.3. The purity of $(c_3)_2(\Delta(1-10)r_2)_3$ holoenzyme was quantified by densitometry.

*Overexpression and Purification of Reconstituted Wild-Type Enzyme.* A parallel method of overexpression and purification of the wild-type enzyme was developed. The aspartate transcarbamoylase catalytic and regulatory subunits were overexpressed separately utilizing strain EK1104 containing pEK17 (*23*) and strain EK1104 containing pEK164 (*6*), respectively. Bacteria were cultured at 37 °C with agitation in M9 media (*21*) containing 0.5% casamino acids, 12 $\mu$g/mL uracil, and 150 $\mu$g/mL ampicillin. Cells were harvested and resuspended in 0.1 M Tris-HCl buffer, pH 9.2, followed by sonication to lyse the cells. Reconstitution of the holoenzyme was achieved by mixing crude cell extracts from the cells expressing the catalytic and regulatory subunits using excess regulatory subunit at 4 °C for 16 h in 50 mM Tris−acetate buffer, 2 mM 2-mercaptoethanol, and 0.1 mM zinc acetate at pH 8.3. Holoenzyme formation was monitored by nondenaturing PAGE. Purification of the reconstituted enzyme was achieved first by precipitation of the holoenzyme at its isoelectric point (*9*) followed by ion-exchange chromatography using Q-Sepharose Fast Flow resin (*29*). After concentration of the reconstituted wild-type enzyme, the purity of the enzyme was checked by SDS−PAGE.

*Determination of Protein Concentration.* The concentrations of the reconstituted wild-type and the $(c_3)_2(\Delta(1-10)r_2)_3$ holoenzyme were determined by the Bio-Rad version of Bradford's dye binding assay (*3*) with wild-type enzyme as a standard.

*Aspartate Transcarbamoylase Assay.* The aspartate transcarbamoylase activity was measured at 25 °C by the colorimetric method (*25*). The saturation curves for aspartate, ATP, CTP, and UTP were performed in duplicate, and data points shown in the figures are the average values. Assays were performed in 0.05 M Tris−acetate buffer, pH 8.3, or in 0.1 M imidazole−acetate buffer, pH 7.0. Data analysis of the steady-state kinetics was carried out as previously described (*28*). Nucleotide saturation curves for the $(c_3)_2(\Delta(1-10)r_2)_3$ holoenzyme in 0.1 M imidazole−acetate, pH 7.0, exhibited dual effects, both activation and inhibition. Therefore, data in Figures 5 and 6 were fit to a function that was composed of a component for hyperbolic inhibition plus a component for hyperbolic activation.

## RESULTS

*Overexpression and Purification of the $(c_3)_2$ $(\Delta(1-10)r_2)_3$ Holoenzyme.* Expression of the $(c_3)_2(\Delta(1-10)r_2)_3$ holoenzyme was attempted first using the *pyrB* promoter. The precipitation of the $(c_3)_2(\Delta(1-10)r_2)_3$ holoenzyme with the cell debris made the mutant enzyme difficult to purify. Analysis of the cell extracts of EK1104/pEK303 by nondenaturing PAGE indicated poor overexpression of the $(c_3)_2(\Delta(1-10)r_2)_3$ holoenzyme. While SDS−PAGE indicated expression of the catalytic chain, the regulatory chain was not expressed in stoichiometric amounts.

However, the $(c_3)_2$ $\Delta(1-10)r_2)_3$ holoenzyme was formed in good yield by mixing $\Delta(1-10)r_2$ with $c_3$. When the $\Delta(1-10)r_2$ was mixed with wild-type $c_3$, a precipitate formed. The supernatant and precipitate were characterized by nondenaturing PAGE; the majority of the mutant enzyme

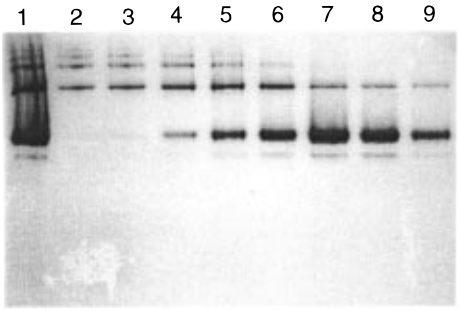


FIGURE 2: The $(c_3)_2(\Delta(1-10)r_2)_3$ high molecular weight aggregate and holoenzyme were separated by sucrose gradient centrifugation. Ten microliters of pregradient $(c_3)_2(\Delta(1-10)r_2)_3$ aggregate (lane 1) and fractions 9 (lane 2), 11 (lane 3), 15 (lane 4), 19 (lane 5), 23 (lane 6), 25 (lane 7), 27 (lane 8), 29 (lane 9), and 33 (lane 10) was analyzed by nondenaturing polyacrylamide gel electrophoresis [6% acrylamide, 0.16% *N*,*N*′-methylene-bis-acrylamide] and stained with Coomassie Brilliant Blue 250.

was in the precipitate whereas trace amounts remained in the supernatant. When the same samples were analyzed by SDS−PAGE, two protein bands were observed. One band corresponded to the catalytic chain, $M_r$ 34 000, and a second band, which had migrated slightly farther than the wild-type regulatory chain, $M_r$ 17 000, corresponded to $\Delta(1-10)r_2$. Analysis by nondenaturing PAGE showed a major band, the $(c_3)_2(\Delta(1-10)r_2)_3$ holoenzyme, which corresponded to the wild-type holoenzyme. Aspartate transcarbamoylase normally forms high molecular weight species which can be identified on a nondenaturing polyacrylamide gel. The $(c_3)_2(\Delta(1-10)r_2)_3$ aggregate formed this high molecular weight species as identified on nondenaturing PAGE; in addition, several other higher molecular weight species formed as identified by several other bands present on the nondenaturing PAGE. Since SDS−PAGE indicated that there were no other protein species present besides the catalytic chain and the $\Delta(1-10)r_2$, the extraneous bands on the nondenaturing PAGE most likely correspond to a series of high molecular weight aggregates of $(c_3)_2(\Delta(1-10)r_2)_3$.

Addition of the nucleotides CTP, CDP, ATP, ADP, AMP, or UTP solubilized the aggregate although the high molecular weight species remained in solution. To separate the $(c_3)_2(\Delta(1-10)r_2)_3$ holoenzyme from the high molecular weight aggregates, a sucrose gradient was utilized; the gradient was effective in purifying the $(c_3)_2(\Delta(1-10)r_2)_3$ holoenzyme from the high molecular weight aggregates (Figure 2). After sucrose gradient purification, the enzyme was approximately 90% $(c_3)_2(\Delta(1-10)r_2)_3$ holoenzyme with the remainder being high molecular weight aggregate and $(c_3)_2(\Delta(1-10)r_2)_2$, whereas prior to the sucrose gradient the $(c_3)_2(\Delta(1-10)r_2)_3$ holoenzyme composed less than 50% of the $(c_3)_2(\Delta(1-10)r_2)_3$ mixture.

*Steady-State Kinetics of the Reconstituted Wild-Type and $(c_3)_2\,\Delta(1-10)r_2)_3$ Holoenzymes.* The reconstituted wild-type enzyme exhibited kinetic parameters almost identical to holoenzyme purified by the standard method (*23*). Therefore, any alterations in the kinetics of the $(c_3)_2(\Delta(1-10)r_2)_3$ holoenzyme should be due to the deletion and not the reconstitution. Sigmoidal kinetics were observed at pH 8.3 and pH 7.0 for the $(c_3)_2(\Delta(1-10)r_2)_3$ holoenzyme (Figure 3). The maximal observed specific activity of the $(c_3)_2(\Delta(1-10)r_2)_3$ holoenzyme at pH 8.3 was 18% lower and at pH 7.0 was 20% lower than the reconstituted wild-type enzyme

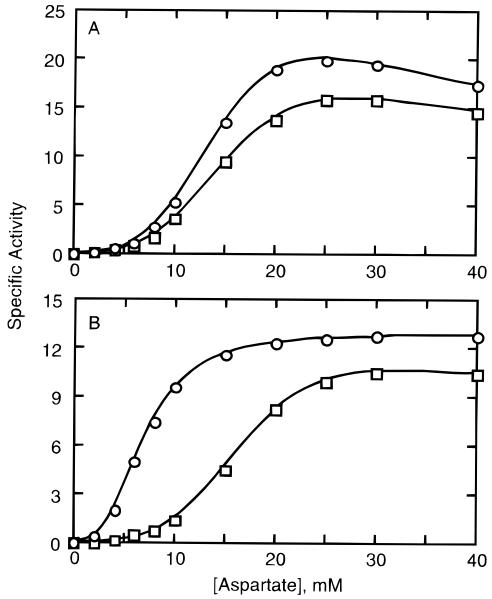


FIGURE 3: Aspartate saturation curves of reconstituted wild-type (○) and $(c_3)_2(\Delta(1-10)r_2)_3$ holoenzyme (□). Specific activity is reported in millimoles of *N*-carbamoyl-L-aspartate formed per hour per milligram of protein. Colorimetric assays were performed at 25 °C at saturating concentrations of carbamoyl phosphate (4.8 mM) in (A) 0.05 M Tris−acetate buffer, pH 8.3, and (B) 0.1 M imidazole−acetate buffer, pH 7.0.

Table 1: Kinetic Parameters of the Reconstituted Wild-Type and Mutant Holoenzymes

| enzyme | max velocity[a] (mmol·h$^{-1}$·mg$^{-1}$) | $[Asp]_{0.5}$ (mM) | $n_H$ |
|---|---|---|---|
| | pH 8.3[b] | | |
| reconstituted wild-type | 18.4 ± 1.5[c] | 12.0 ± 0.6 | 2.4 ± 0.3 |
| $(c_3)_2(\Delta(1-10)r_2)_3$ | 14.9 ± 1.0 | 15.2 ± 1.0 | 3.0 ± 0.3 |
| | pH 7.0[d] | | |
| reconstituted wild-type | 13.2 ± 1.6 | 7.1 ± 0.7 | 2.1 ± 0.5 |
| $(c_3)_2(\Delta(1-10)r_2)_3$ | 10.4 ± 1.3 | 14.2 ± 1.2 | 2.7 ± 0.3 |

[a] The maximal velocity represents the maximal observed specific activity from the aspartate saturation curve. [b] These data were determined from the aspartate saturation curves (Figure 2). Colorimetric assays were performed at 25 °C in 0.05 M Tris−acetate buffer, pH 8.3, and saturating levels of carbamoyl phosphate (4.8 mM). [c] These data were determined from the aspartate saturation curves. Colorimetric assays were performed at 25 °C in 0.1 M imidazole−acetate buffer, pH 7.0, and saturating levels of carbamoyl phosphate (4.8 mM). [d] Average deviation of three determinations.

(Table 1). The aspartate concentration at half the maximal observed activity ($[Asp]_{0.5}$) was 1.5-fold greater at pH 8.3 and 2-fold greater at pH 7.0 than the values for the reconstituted wild-type holoenzyme. The Hill coefficient ($n_H$) for the $(c_3)_2(\Delta(1-10)r_2)_3$ holoenzyme at pH 8.3 and pH 7.0 was slightly greater than the $n_H$ of the reconstituted wild-type enzyme (Table 1).

*Response of the $(c_3)_2(\Delta(1-10)r_2)_3$ Holoenzyme to the Nucleotide Effectors at pH 8.3.* The heterotropic effects induced by the nucleotides CTP, ATP, and UTP on the wild-type and $(c_3)_2(\Delta(1-10)r_2)_3$ holoenzyme were determined at half $[Asp]_{0.5}$ (Table 2). The concentrations of nucleotide required to half-inhibit ($K_{CTP}$) or half-activate ($K_{ATP}$) were also determined. CTP inhibits the $(c_3)_2(\Delta(1-10)r_2)_3$ holoenzyme to the same extent as the reconstituted wild-type holoenzyme, but it bound with an apparent affinity an order of magnitude higher (Figure 4). The $(c_3)_2(\Delta(1-10)r_2)_3$

Table 2: CTP Inhibition and ATP Activation of the Reconstituted Wild-Type and Mutant Holoenzymes at Subsaturating Aspartate at pH 8.3[a]

| CTP Parameters | | |
|---|---|---|
| enzyme | residual activity (%)[b] | $K_{CTP}$[c] (mM) |
| reconstituted wild-type | 14.5 ± 1.4[d] | 0.019 ± 0.0004 |
| $(c_3)_2(\Delta(1-10)r_2)_3$ | 17.8 ± 6.6 | 0.0051 ± 0.001 |
| **ATP Parameters** | | |
| enzyme | % activation[e] | $K_{ATP}$ (mM) |
| reconstituted wild-type | 533.7 ± 54.0 | 1.1 ± 0.1 |
| $(c_3)_2(\Delta(1-10)r_2)_3$ | 262.0 ± 35.5 | 1.9 ± 0.002 |

[a] These data were determined from ATP and CTP saturation curves (Figure 3). Colorimetric assays were performed at 25 °C in 0.05 M Tris−acetate buffer, pH 8.3. ATP and CTP saturation curves were determined at saturation levels of carbamoyl phosphate (4.8 mM) and aspartate concentrations at half the $[Asp]_{0.5}$ of the respective holoenzyme at pH 8.3. [b] Percent residual activity is defined as $100[(A - A_{CTP})/A]$ where $A_{CTP}$ is the activity in the presence of CTP and $A$ is the activity in the absence of CTP. [c] $K$ is the nucleotide concentration required to activate or inhibit the enzyme by 50% of the maximal effect. [d] Average deviation of three determinations. [e] Percent activation is defined as $100[(A_{ATP} - A)/A]$ where $A_{ATP}$ is the activity in the presence of ATP and $A$ is the activity in the absence of ATP.

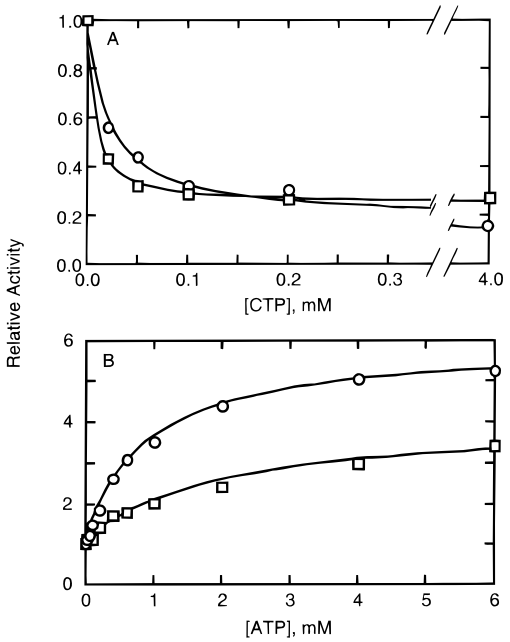


FIGURE 4: Influence of CTP (A) and ATP (B) on the activity of reconstituted wild-type (○) and $(c_3)_2(\Delta(1-10)r_2)_3$ holoenzyme (□). The colorimetric assays were performed at 25 °C in 0.05 M Tris−acetate buffer, pH 8.3, at saturating concentrations of carbamoyl phosphate (4.8 mM). The aspartate concentration was held constant at half the $[Asp]_{0.5}$.

holoenzyme was activated by ATP, but the maximal activation was 50% less than the reconstituted wild-type enzyme (Figure 4). ATP bound to the $(c_3)_2(\Delta(1-10)r_2)_3$ holoenzyme with 75% less apparent affinity than the reconstituted wild-type enzyme. UTP did not activate or inhibit the reconstituted wild-type or the $(c_3)_2(\Delta(1-10)r_2)_3$ holoenzyme under these conditions.

*Response of the Mutant Enzyme to the Nucleotide Effectors at pH 7.0.* The heterotropic effects of CTP, ATP, UTP, and CTP + UTP were also determined at pH 7.0. At pH 7.0, UTP inhibits the enzyme in the absence and presence of CTP (*34*); this is not observed at pH 8.3. At pH 7.0, the

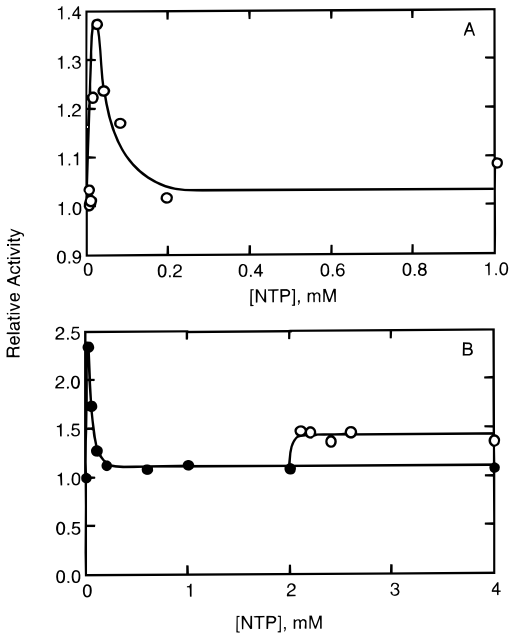


FIGURE 5: (A) Influence of CTP (○) on the activity of $(c_3)_2(\Delta(1-10)r_2)_3$ holoenzyme. (B) Influence of CTP (●) and CTP in the presence of UTP (○) on the activity of $(c_3)_2(\Delta(1-10)r_2)_3$ holoenzyme. The colorimetric assays were performed at 25 °C in 0.1 M imidazole−acetate, buffer pH 7.0, at saturating concentrations of carbamoyl phosphate (4.8 mM). The aspartate concentration was held constant at half the $[Asp]_{0.5}$.

nucleotides also bind with greater affinity. The response of the $(c_3)_2(\Delta(1-10)r_2)_3$ holoenzyme to the nucleotides was more complex than for the wild-type enzyme at pH 7.0. Reconstituted wild-type enzyme was inhibited by CTP, slightly inhibited by UTP, and activated by ATP. Low concentrations of CTP activated the $(c_3)_2(\Delta(1-10)r_2)_3$ holoenzyme. As the concentration of CTP increased, inhibition was observed; however, a slight activation of the $(c_3)_2(\Delta(1-10)r_2)_3$ holoenzyme was the overall effect (Figure 5). ATP inhibited the $(c_3)_2(\Delta(1-10)r_2)_3$ holoenzyme at low nucleotide concentrations, followed by activation as the concentration of the respective nucleotide was increased (Figure 6). At high concentrations of ATP, there was an overall activation of the enzyme. UTP activated the mutant enzyme. All three nucleotides bind with greater apparent affinity to the $(c_3)_2(\Delta(1-10)r_2)_3$ holoenzyme as compared to the wild-type enzyme.

*Competition Studies between UTP and CTP.* At pH 7.0, UTP in the presence of CTP synergistically inhibits wild-type aspartate transcarbamoylase (*34*), as well as the reconstituted wild-type enzyme prepared here. However, CTP plus UTP saturation curves of the $(c_3)_2(\Delta(1-10)r_2)_3$ holoenzyme showed no synergistic inhibition (Figure 5). At saturating CTP, the $(c_3)_2(\Delta(1-10)r_2)_3$ holoenzyme was slightly activated, and the addition of UTP did not produce synergistic inhibition.

The UTP effects on the $(c_3)_2(\Delta(1-10)r_2)_3$ holoenzyme in the presence of varying amounts of CTP, 0.002−2.0 mM, were investigated (data not shown). As the amount of CTP held constant was increased, the level of activation by UTP decreased until at saturating CTP (2 mM) there was no UTP effect.

*Competition Studies between UTP and ATP.* The effects of UTP on the activity of the $(c_3)_2(\Delta(1-10)r_2)_3$ holoenzyme

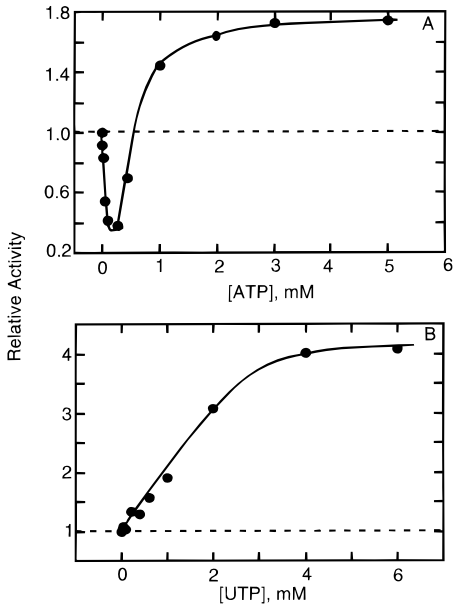


FIGURE 6: Influence of ATP (A) and UTP (B) on the activity of $(c_3)_2(\Delta(1-10)r_2)_3$ holoenzyme. The colorimetric assays were performed at 25 °C in 0.1 M imidazole−acetate, pH 7.0, at saturating concentrations of carbamoyl phosphate (4.8 mM). The aspartate concentration was held constant at half the $[Asp]_{0.5}$.

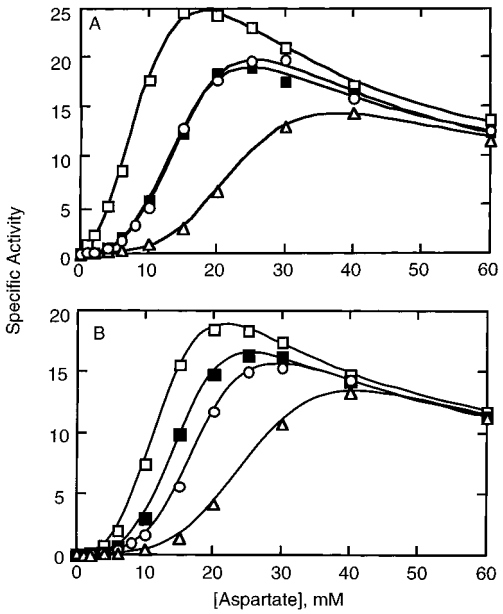


FIGURE 7: Aspartate saturation curves of reconstituted wild-type (A) and $(c_3)_2(\Delta(1-10)r_2)_3$ holoenzyme (B) without effector (○) and in the presence of 2 mM ATP (□), 2 mM CTP (△) and 2 mM UTP (■). The colorimetric assays were performed at 25 °C in 0.05 M Tris−acetate buffer, pH 8.3, at saturating concentrations of carbamoyl phosphate (4.8 mM).

at pH 7.0 were investigated using UTP saturation assays in the presence of ATP (data not shown). In a series of experiments, the ATP concentration was held constant (0.2−2.0 mM) while UTP was titrated up to 8 mM. Regardless of the concentration of ATP present, UTP activated the $(c_3)_2(\Delta(1-10)r_2)_3$ holoenzyme to the same extent, although greater concentrations of UTP were required to displace the higher concentrations of ATP. This effect indicated that UTP activates the $(c_3)_2(\Delta(1-10)r_2)_3$ holoenzyme and competes with ATP for the same binding site.

*Aspartate Saturation Curves in the Presence and Absence of Nucleotide Effectors of the Reconstituted Wild-Type and $(c_3)_2(\Delta(1-10)r_2)_3$ Holoenzymes.* The aspartate saturation curves in the presence of saturating effectors were determined for the $(c_3)_2(\Delta(1-10)r_2)_3$ holoenzyme at pH 8.3, and the shifts in the $[Asp]_{0.5}$ and $n_H$ parameters caused by the effectors were similar to those observed for the reconstituted wild-type enzyme (Figure 7). Aspartate saturation curves of the $(c_3)_2(\Delta(1-10)r_2)_3$ holoenzyme in the presence and absence of effectors at pH 7.0 exhibited activation by all three nucleotide effectors (Figure 8). The maximal observed specific activity was the same for the $(c_3)_2(\Delta(1-10)r_2)_3$ holoenzyme in the presence and absence of the effectors. PALA, a bisubstrate analog, activates the wild-type enzyme since the binding of PALA induces the T to R transition. PALA saturation curves at one-fifth the half-saturation of aspartate for the $(c_3)_2(\Delta(1-10)r_2)_3$ holoenzyme (data not shown) show a greater activation than the wild-type enzyme.

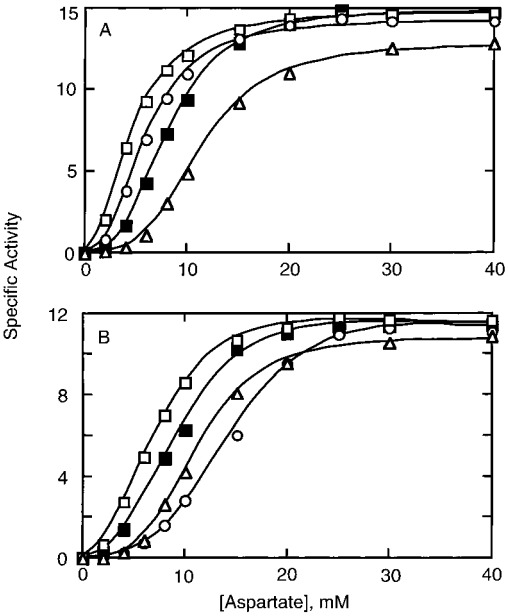


FIGURE 8: Aspartate saturation curves of reconstituted wild-type (A) and $(c_3)_2(\Delta(1-10)r_2)_3$ holoenzyme (B) without effector (○) and in the presence of 2 mM ATP (□), 2 mM CTP (△) and 2 mM UTP (■). The colorimetric assays were performed at 25°C in 0.1 M imidazole−acetate buffer, pH 7.0, at saturating concentrations of carbamoyl phosphate (4.8 mM).

## DISCUSSION

The role of the N-terminal region of the regulatory chain of aspartate transcarbamoylase has been uncertain since its position has not been well-defined in the structure due to poor electron density (*14*, *16*, *30*). Previous studies have proposed that the N-terminal region has direct interactions with the nucleotide effectors, stabilizes the 80r's loop, orients the S1′ $\beta$-strand, and forms R1−R6 interactions, thereby coupling the allosteric binding sites within the dimer (*15*, *16*, *30*). Mutagenesis of residues Thr-2r through Leu-7r suggested that these residues may play a role in the heterotropic mechanism, especially those involving UTP effects (*7*). In this work the deletion of amino acids 1−10 from the regulatory chain and the subsequent examination of the $(c_3)_2(\Delta(1-10)r_2)_3$ holoenzyme have elucidated more information concerning the structural and functional role of the N-terminal region of aspartate transcarbamoylase.

The N-terminal region is important for the monomeric structure of the aspartate transcarbamoylase holoenzyme. The $(c_3)_2(\Delta(1-10)r_2)_3$ holoenzyme is produced *in vivo* under control of the *pyrBI* promoter but could not be purified successfully by standard methods since the $(c_3)_2(\Delta(1-10)r_2)_3$ holoenzyme forms a high molecular weight aggregate which precipitates out of solution. Since CTP can solubilize the aggregate, it is likely that the nucleotide site is involved in the formation of the aggregate. Therefore, the N-terminal region blocks an area of the protein from interacting with an attractive site on another $(c_3)_2(\Delta(1-10)r_2)_3$ holoenzyme, thereby preventing aggregation.

*N-Terminal Region Stabilizes the Enzyme Conformation.* The sigmoidal kinetic parameters of the mutant holoenzyme are similar to the wild-type enzyme and suggest that the catalytic mechanism was unaffected. Despite being 60 Å away from the active site, deletion of the N-terminal region of the regulatory chain does have a slight effect on the homotropic properties. The wild-type enzyme undergoes the T to R conformational change by the binding of aspartate to the active site. The equilibrium between the T and R states appears to be shifted toward the T-state for the $(c_3)_2(\Delta(1-10)r_2)_3$ holoenzyme compared to the wild-type enzyme since a higher concentration of aspartate is required to promote the T to R conformational change.

Studies have been performed to test the hypothesis that global free energy changes are responsible for the transmission of the homotropic and heterotropic mechanisms in aspartate transcarbamoylase (*1*). One explanation of the effects of the mutant enzymes investigated in that study (*1*) was that the mutations alter the global stabilization of either the T or the R state of the enzyme. Deletion of the N-terminal region affects the homotropic mechanism and may shift the equilibrium between the T and R states, which suggests that the N-terminal region stabilizes the enzyme conformation. Therefore, the N-terminal region is important for the monomeric form of the holoenzyme and may be important for the relative stability of the T and R states.

*N-Terminal Region Interactions Effecting CTP and ATP Binding and Heterotropic Effects.* Upon removal of the N-terminal region, CTP binds with greater affinity to the mutant enzyme but has slightly less of an inhibitory effect at pH 8.3. Therefore, in the wild-type holoenzyme, the N-terminal region may regulate CTP and other nucleotide binding, thereby exerting control over inhibition/activation of the enzyme. The N-terminal region may actually hinder the binding of CTP.

Based upon crystallographic data, the N-terminal region has one direct contact with CTP; the carbonyl oxygen of Val-9r hydrogen bonds with the 2′-OH of CTP. ATP, on the other hand, has several contacts between $C_{2'}$ and $O_{2'}$ and the backbone carbonyl of Val-9, $N_3$ and $C_2$ with the backbone carbonyl of Glu-10, and $N_1$ with the Cα of Ala-11 (*30*). ATP also has direct contacts with the S1′ β-strand which is oriented by the N-terminal region (*16*). At pH 8.3, ATP binds with lower apparent affinity to the $(c_3)_2(\Delta(1-10)r_2)_3$ holoenzyme compared to the wild-type enzyme; therefore, these interactions may be important for ATP binding and activation of the holoenzyme. Since there are more interactions between ATP and the N-terminal region compared to the interactions between CTP and the N-terminal region, the observed loss in the apparent ATP affinity and nucleotide response is not unexpected. ATP binding also induces a larger rearrangement of the nucleotide binding pocket than CTP; the removal of the N-terminal region may affect the heterotropic effect of ATP since the N-terminal region may play a role in the expansion of the binding pocket and the heterotropic effect. The data at pH 7.0 suggest that the N-terminal region of the regulatory subunit is important for ATP binding and subsequent activation of the wild-type holoenzyme.

*N-Terminal Region Links the R1 Binding Site to the R6 Binding Site.* It has been proposed that the nucleotide binding sites within one dimer are coupled by the N-terminal region (*15*). Thus, communication between each binding site and the heterotropic effect may be facilitated partly through the N-terminal region. Deletion of the first 10 residues of the regulatory chain may alter part of the R1−R6 interface which would explain the altered nucleotide effects seen in the $(c_3)_2(\Delta(1-10)r_2)_3$ holoenzyme. At pH 7.0, each nucleotide exhibits both inhibition and activation which may not be observed at pH 8.3 due to weaker binding; this dual effect may be due to a decoupling of the nucleotide binding sites. The deletion of the N-terminal region may create two distinct binding sites, an activation (A) site and an inhibition (I) site, which have limited communication. The nucleotides bind to one site with greater affinity than the other, thus the initial response of the enzyme. Upon binding of nucleotide to the second site and saturation of the binding sites, the overall effect is seen.

CTP binds with greater affinity to the A site; therefore, activation of the enzyme is observed first. As CTP binds to the second site, the I site, inhibition of the enzyme occurs which results in an overall slight activation. Similar to CTP, ATP binds with greater affinity to one site, the I site, and inhibition is observed first. As ATP binds to the second site, the A site, the inhibitory effects are reversed and activation of the enzyme occurs. When the binding sites are saturated with ATP, an overall activation of the enzyme occurs. These results suggest that the R1 and R6 binding sites are asymmetrical and that the N-terminal region is necessary for communication between the two sites.

*N-Terminal Region Interacts with UTP and Creates Asymmetrical Binding Sites within the Dimer.* The UTP saturation curve at pH 7.0 of the $(c_3)_2(\Delta(1-10)r_2)_3$ holoenzyme has a response similar to ATP which is the opposite of the wild-type enzyme. Direct interactions with the N-terminal region and alignment of the S1′ β-strand are important for UTP recognition and the subsequent effects as seen with the N-terminal alanine scanning mutations (*7*). UTP in the presence of CTP at pH 7.0 synergistically inhibits the wild-type enzyme (*34*); however, this is not the case for the $(c_3)_2(\Delta(1-10)r_2)_3$ holoenzyme. These results, along with the ATP plus UTP competition studies, indicate UTP no longer binds preferentially to the low-affinity site, but to the high-affinity site. This suggests that the N-terminal region has important direct interactions with UTP and forms part of the asymmetry responsible for creating the low- and high-affinity binding sites. Residues within the N-terminal region may be important for discrimination between CTP and UTP due to direct interactions as well as the asymmetry between the R1 and the R6 binding sites. The asymmetry in the R1 and R6 binding sites may create the high-affinity and low-affinity sites which discriminate between CTP and UTP.

*Conclusions.* Removal of residues 1−10 of the regulatory chain N-terminal region creates an enzyme which exhibits altered solubility properties and differs functionally from the wild-type enzyme. Foremost, the N-terminal region covers an area which interacts in an attractive manner to another site on the enzyme; this interaction decreases the holoenzyme's solubility. Removal of this region may create a conformational change in the quaternary structure of the enzyme resulting in a shift in the T to R equilibrium. The N-terminal region is also important for controlling the binding of the nucleotide effectors, orienting other residues in the binding site and the subsequent heterotropic response. This region helps distinguish the R1 binding site, from the R6 binding site, creating the high- and low-affinity binding sites and coupling these binding sites within the regulatory dimer.

## ACKNOWLEDGMENT

We thank Dr. Mark Williams for the preparation of EK1595. We also thank Dr. Williams and Dr. Boguslaw Stec for many helpful discussions.

## REFERENCES

1. Aucoin, J. M., Pishko, E. J., Baker, D. P., and Kantrowitz, E. R. (1996) *J. Biol. Chem. 271*, 29865−29869.
2. Baker, D. P., and Kantrowitz, E. R. (1993) *Biochemistry 32*, 10150−10158.
3. Bradford, M. M. (1976) *Anal. Biochem. 72*, 248−254.
4. Changeux, J.-P., Gerhart, J. C., and Schachman, H. K. (1968) *Biochemistry 7*, 531−538.
5. Davis, B. J. (1964) *Ann. N.Y. Acad. Sci. 121*, 404−427.
6. Dembowski, N. J., and Kantrowitz, E. R. (1993) *Protein Eng. 6*, 123−127.
7. Dembowski, N. J., and Kantrowitz, E. R. (1994) *Protein Eng. 7*, 673−679.
8. Evans, S. V. (1993) *J. Mol. Graphics 11*, 134−138.
9. Gerhart, J. C., and Holoubek, H. (1967) *J. Biol. Chem. 242*, 2886−2892.
10. Gerhart, J. C., and Pardee, A. B. (1962) *J. Biol. Chem. 237*, 891−896.
11. Gerhart, J. C., and Pardee, A. B. (1962) *J. Biol. Chem. 237*, 891−896.
12. Gerhart, J. C., and Pardee, A. B. (1963) *Cold Spring Harbor Symp. Quant. Biol. 28*, 491−496.
13. Gouaux, J. E., Stevens, R. C., and Lipscomb, W. N. (1990) *Biochemistry 29*, 7702−7715.
14. Honzatko, R. B., Crawford, J. L., Monaco, H. L., Ladner, J. E., Edwards, B. F. P., Evans, D. R., Warren, S. G., Wiley, D. C., Ladner, R. C., and Lipscomb, W. N. (1982) *J. Mol. Biol. 160*, 219−263.
15. Honzatko, R. B., and Lipscomb, W. N. (1982) *J. Mol. Biol. 160*, 265−286.
16. Kosman, R. P., Gouaux, J. E., and Lipscomb, W. N. (1993) *Proteins: Struct. Funct., Genet. 15*, 147−176.
17. Krause, K. L., Voltz, K. W., and Lipscomb, W. N. (1987) *J. Mol. Biol. 193*, 527−553.
18. Kunkel, T. A. (1985) *Proc. Natl. Acad. Sci. U.S.A. 82*, 488−492.
19. Ladjimi, M. M., Ghellis, C., Feller, A., Cunin, R., Glansdorff, N., Pierard, A., and Hervé, G. (1985) *J. Mol. Biol. 186*, 715−724.
20. Laemmli, U. K. (1970) *Nature (London) 227*, 680−685.
21. Maniatis, T., Fritsch, E. F., and Sambrook, J. (1982) in *Molecular Cloning*, pp 368−369, Cold Spring Harbor Laboratory, New York.
22. Monaco, H. L., Crawford, J. L., and Lipscomb, W. N. (1978) *Proc. Natl. Acad. Sci. U.S.A. 75*, 5276−5280.
23. Nowlan, S. F., and Kantrowitz, E. R. (1985) *J. Biol. Chem. 260*, 14712−14716.
24. Ornstein, L. (1964) *Ann. N.Y. Acad. Sci. 121*, 321−349.
25. Pastra-Landis, S. C., Foote, J., and Kantrowitz, E. R. (1981) *Anal. Biochem. 118*, 358−363.
26. Robey, E. A., and Schachman, H. K. (1985) *Proc. Natl. Acad. Sci. U.S.A. 82*, 361−365.
27. Sanger, F., Nicklen, S., and Coulson, A. R. (1977) *Proc. Natl. Acad. Sci. U.S.A. 74*, 5463−5467.
28. Silver, R. S., Daigneault, J. P., Teague, P. D., and Kantrowitz, E. R. (1983) *J. Mol. Biol. 168*, 729−745.
29. Stebbins, J. W., and Kantrowitz, E. R. (1989) *J. Biol. Chem. 264*, 14860−14864.
30. Stevens, R. C., Gouaux, J. E., and Lipscomb, W. N. (1990) *Biochemistry 29*, 7691−7701.
31. Studier, F. W., Rosenberg, A. H., Dunn, J. J., and Duberndorff, J. W. (1990) *Methods Enzymol. 185*, 60−89.
32. Vieira, J., and Messing, J. (1987) *Methods Enzymol. 153*, 3−11.
33. Wente, S. R., and Schachman, H. K. (1987) *Proc. Natl. Acad. Sci. U.S.A. 84*, 31−35.
34. Wild, J. R., Loughrey-Chen, S. J., and Corder, T. S. (1989) *Proc. Natl. Acad. Sci. U.S.A. 86*, 46−50.

BI972102G